Wave packet diffraction in the Kronig–Penney model

2002 J. Phys. A: Math. Gen. 35 1045

(http://iopscience.iop.org/0305-4470/35/4/316)

INSTITUTE OF PHYSICS PUBLISHING JOURNAL OF PHYSICS A: MATHEMATICAL AND GENERAL

J. Phys. A: Math. Gen. **35** (2002) 1045–1053 PII: S0305-4470(02)27462-4

Wave packet diffraction in the Kronig–Penney model

G Kälbermann

Soil and Water Department, Faculty of Agriculture, Rehovot 76100, Israel

E-mail: hope@vms.huji.ac.il

Received 30 July 2001, in final form 22 November 2001
Published 18 January 2002
Online at stacks.iop.org/JPhysA/35/1045

Abstract
The phenomenon of wave packet diffraction in space and time is investigated numerically and analytically for a one-dimensional array of equally spaced finite-depth wells. Theoretical predictions for the lattice at long times and at low scattering energies coincide exactly with the results for a single well. At intermediate and short times compared to the classical passage time, the pattern shows both a broad diffractive pattern and an interference pattern inside each diffractive peak. The diffractive structure persists for this case to infinite time.

PACS numbers: 03.65.Nk, 03.65.Pm, 03.80.+r

1. Introduction

The phenomenon of wave packet diffraction in space and time was found numerically in one and two dimensions [1, 2] and treated analytically in one and three dimensions at long times [3]. The effect appears in wave packet matter waves potential scattering for the nonrelativistic Schrödinger equation, as well as for the relativistic Dirac equation.

The essence of this recently found effect is the production of a multiple-peak diffractive structure that travels in space. The pattern is not stationary, but it progresses with time. The pattern broadens and diminishes in amplitude in order to conserve flux, but, it preserves its shape structure. The peaks do not mingle or cross each other. Interference between the incoming and spreading wave packet and the scattered wave is deemed to be responsible for the multiple peak structure.

This structure exists for all packets but it survives to infinite time only for packets that are initially narrower than a value related to the potential width (see section 2). For wider packets the peak structure merges into a single peak. The effect is named *wave packet diffraction in space and time*.

The pattern is produced by a time-independent potential. The time dependence of the diffraction pattern is due to the progress of the packet. A plane wave, being stationary in time, does not reveal such behaviour. For plane monochromatic waves quantum scattering displays diffraction phenomena in time [4] induced by the sudden opening of a slit, or in space by fixed slits or gratings. The combined effect of time-dependent opening of slits for plane monochromatic waves produces diffraction patterns in space and time [5]. These patterns *fade out* asymptotically in time. Recent measurements of atomic wave diffraction [6], have indeed demonstrated that the *diffraction in time* process is supported by experiments.

It was found in [1–3] that there is no need to have a sudden (time-dependent) opening of a slit to generate a time-dependent diffractive train. The multiple-peak travelling structure is generated by a time-independent potential provided the packet width is narrower than the extent of the potential of either the well or the barrier. The time-dependent behaviour stems from the time-dependent spreading and motion of the initial and scattered packets.

This is the major difference between diffraction in space and time with plane monochromatic waves and wave packet diffraction in space and time. For monochromatic waves the time dependence arises from the time variation of the obstacles, like the opening or shutting of slits, whereas for wave packets the potentials are fixed and time independent. Consequently, the packet diffraction patterns survive to infinite time while their monochromatic counterparts do not. The only restriction for the occurrence of such behaviour is the production of wave packets that are initially narrower than a size determined by the dimensions of the potential extent and the impinging average momentum of the packet. The effect awaits experimental confirmation. In [3] a hypothetical experiment with liquid helium below the λ transition was simulated. The simulation showed that the travelling diffractive structure will appear in such an experiment as large oscillations with time in the amount of helium atoms receding from an impervious wall. It was assumed in the simulation that the wall behaved in the same manner as a single scatterer, in the hope that a strong enough repulsive barrier provided by the first line of atoms in the impervious wall is the all-important factor in the production of the patterns. This concept was not demonstrated either analytically or numerically. Any target, be it a foil that is irradiated by some beam, or a quantum well or heterostructure scattering a current, involves a large array of scatterers. The purpose of the present paper is to address the problem of wave packet diffraction in the context of a one-dimensional array of equally spaced finite size and fine depth wells, as the time-honoured Kronig–Penney model [7]. This investigation is aimed at showing that the tacit assumption of [3] is correct. A large array of scatterers behaves very similar to the single potential. Differences will arise in the fine structure of the patterns as will be depicted in section 4.

We treat the case of a finite size array and not an infinite one. Therefore, Bloch's theorem will not be of help in dealing with it. The appearance of the phenomenon we aim at depends on the spatial extent of the wells. The δ function type of potentials will not produce a diffraction pattern with wave packets. Despite the complications arising from the use of a finite number of finite size wells, the outcome of the scattering events will turn out to be quite independent of the number of wells, their depth, etc. The only aspect that will matter crucially is the width of a single well in the array. In section 2 we briefly review some needed results of [3]. Section 3 deals with the Kronig–Penney model analytically and section 4 numerically. Section 5 summarizes the paper.

2. Wave packet diffraction in space and time

In [3] we found that for $t \to \infty$ it is possible to write analytical formulae for the diffraction pattern produced by a scattering event of a wave packet at a well or barrier. The formulae were derived for the simplest possible case that can be dealt with almost completely analytically.

This is the example of a wave packet scattering off a square well in one and three dimensions. The results, however, were shown to be independent of the shape of the well and the packet.

As it is our intention to treat the one-dimensional array of wells, we recapitulate here the one-dimensional formula as a bridge to the lattice case.

Consider a Gaussian wave packet impinging from the left on a well located around the origin,

$$V(x) = -V_0\,\Theta(w/2 - |x|) \tag{1}$$

where w is the width, Θ the Heaviside function and V_0 the depth. Using the results of [8] the reflected and transmitted packets become

$$\psi(x,t) = \int_{-\infty}^{\infty} \phi(k,x,t)\, a(k,q_0) \exp\left(-\mathrm{i}\frac{k^2}{2m}t\right)\mathrm{d}k \tag{2}$$

where $\phi(k, x, t)$ is the stationary solution to the square-well scattering problem for each k and $a(k, q_0)$ is the Fourier transform amplitude for the initial wavefunction with an average momentum q_0.

As the effect is due to the interference between the incoming spread packet and the reflected wave we focus on the backward direction for $x < -w/2$

$$\begin{aligned}
&\phi(k,x,t) = D(k,k')\,\mathrm{e}^{\mathrm{i}k(x-x_0)} + F(k,k')\,\mathrm{e}^{-\mathrm{i}k(x+x_0+2w)}\\
&D(k,k') = 1\\
&F(k,k') = \frac{E(k,k')}{A(k,k')}\\
&E(k,k') = -2\,\mathrm{i}\,(k^2 - k'^2)\sin(2k'w)\\
&A(k,k') = (k+k')^2\mathrm{e}^{-2\mathrm{i}k'w} - (k-k')^2\mathrm{e}^{2\mathrm{i}k'w}
\end{aligned} \tag{3}$$

where

$$a(k,q_0) = \mathrm{e}^{\mathrm{i}k(x-x_0)-\sigma^2(k-q_0)^2} \tag{4}$$

with $k' = \sqrt{k^2 + 2m|V_0|}$ and σ the width parameter of the packet.

At $k \approx 0$ we have $F \approx -1$. For long times and distances $x \gg x_0 \gg w$ we find using the properties of Gaussian integrals

$$\begin{aligned}
|\psi| &= 2\sqrt{\frac{2m\pi}{t}}\mathrm{e}^{-z}\left|\sin\left(\frac{mx}{t}\left(x_0 + 2\mathrm{i}\sigma^2 q_0\right)\right)\right|\\
&= 2\sqrt{\frac{2m\pi}{t}}\mathrm{e}^{-z}\sqrt{\sin^2\left(\frac{mxx_0}{t}\right) + \sinh^2\left(\frac{2\sigma^2\, q_0 m x}{t}\right)}\\
z &= \sigma^2\left(\frac{m^2\left(x^2 + x_0^2\right)}{t^2} + q_0^2\right).
\end{aligned} \tag{5}$$

This expression represents a diffraction pattern that travels in time and persists. In [3] we compared the above expression to the numerical solution. Excellent agreement was found without resorting to any scale factor adjustment (see figure 1 in [3]).

We further derived the condition for the pattern to persist to be

$$\sigma \ll \sqrt{\frac{w}{q_0}}. \tag{6}$$

A relation between the initial width of the packet, the width of the well or barrier and the initial average momentum of the packet. Narrow packets only display the effect.

The key element in obtaining the formula of equation (5) was the replacement of F in equation (3) by the value at threshold, namely $F = -1$. This replacement is valid for long times at which the wild oscillations in the exponentials demand a very low momentum. Due to the fact that this value is independent of the type of well or barrier, the result holds in general for any kind of well or barrier. In all the cases where the reflection coefficient F can be replaced by the value at threshold we obtain a receding multiple-peak coherent wave train or a single hump, depending on the initial width of the packet. This is the essence of the phenomenon of *wave packet diffraction in space and time*.

3. Kronig–Penney scattering

Consider now a one-dimensional array of N square wells of width a to the right of the origin at a distance $\delta + a$ apart from each other. We shift the location of the wells as compared to equation (1) for convenience as

$$V(x) = -V_0 \sum_{n=0}^{N-1} \Theta\left(\frac{a}{2} - \left|x - l_n - \frac{a}{2}\right|\right) \tag{7}$$

where the left edge of the well is $l_n = n(\delta + a)$ while the right edge is located at $r_n = l_n + a$.

In order to show that this one-dimensional Kronig–Penney lattice of finite size and depth wells yields essentially the same result as a single well, we will expand the reflection coefficient for the lattice to the third order in k.

In order to find the reflection coefficient equivalent to F of equation (3) we have to solve for the wavefunction as a function of k by means of plane waves, without resorting to Bloch's theorem that applies only for the infinite array.

For each well we write

$$\begin{aligned} \psi &= A_n \mathrm{e}^{\mathrm{i}kx} + B_n \mathrm{e}^{-\mathrm{i}kx} && r_{n-1} < x < l_n \\ &= C_n \mathrm{e}^{\mathrm{i}\kappa x} + D_n \mathrm{e}^{-\mathrm{i}\kappa x} && l_n < x < r_n \\ &= A_{n+1} \mathrm{e}^{\mathrm{i}kx} + B_{n+1} \mathrm{e}^{-\mathrm{i}kx} && r_n < x < l_{n+1} \end{aligned} \tag{8}$$

with $\kappa = \sqrt{k^2 + 2mV_0}$, m being the mass of the impinging particle. For the last well we demand an outgoing wave, hence $B_N = 0$.

Continuity of the wavefunction and its derivative at the right and left edges of each well gives

$$\begin{aligned} \begin{pmatrix} A_n \\ B_n \end{pmatrix} &= M_n \begin{pmatrix} A_{n+1} \\ B_{n+1} \end{pmatrix} \\ M_n &= \begin{pmatrix} z_1 \mathrm{e}^{\mathrm{i}ka} & -z_2 \mathrm{e}^{-\mathrm{i}k(r_n + l_n)} \\ z_2 \mathrm{e}^{\mathrm{i}k(r_n + l_n)} & z_1^* \mathrm{e}^{-\mathrm{i}ka} \end{pmatrix} \end{aligned} \tag{9}$$

where $z_1 = \cos(\kappa a) - \mathrm{i}\sin(\kappa a)(1 + u^2)/(2u)$, $z_2 = \mathrm{i}\sin(\kappa a)(1 - u^2)/(2u)$ and $u = \frac{k}{\kappa}$.

Due to the strong oscillations of $\mathrm{e}^{-\mathrm{i}\frac{k^2}{2m}t}$ in equation (2) the long time behaviour of the wavefunction is determined by the very low $u = \frac{k}{\kappa}$ regime. We therefore expand the matrices in powers of u. The reflection coefficient F will then be obtained from $F = \frac{B_0}{A_0}$ as a polynomial in u.

For a plane wave stationary solution with no incoming waves from the rightmost edge of the wells and the number of wells $N \gg 2$, we find after some lengthy algebra

$$\begin{aligned}\frac{A_0}{A_n} &= 1 + c_0\lambda + (N-2)\, c_0\lambda(1 - \mathrm{e}^{4ik\delta}) + O(\epsilon^2)\\ \frac{B_0}{A_n} &= -(1 + 2\, c_0\lambda + (N-2)\, c_0\lambda(1 - \mathrm{e}^{4ik\delta})) + O(\epsilon^2)\end{aligned} \tag{10}$$

where $c_0 = \cos(\kappa_0 a)$, $\lambda = -\epsilon/i\,\sin(\kappa_0 a)(1 - e^{2ik\delta})$, $\epsilon = \frac{k}{\kappa_0}$ and $\kappa_0 = \sqrt{2mV_0}$ is real for wells and imaginary for barriers. From the expressions above it is seen that to this order the correction to $F \approx -1$ originates from the term multiplied by $(N-2)$. However, this term is identical for both the expressions above. Therefore, to this order, A_0 and $-B_0$ are almost identical.

We have carried out an expansion to $O(\epsilon^3)$ also. The expression becomes quite involved having some 20 terms each for A_0 and B_0. Even to this order the leading terms still give $F \approx -1$.

The Kronig–Penney lattice displays the same low k behaviour of the reflection coefficient as a single well.

In the light of the results of section 2, it follows that the Kronig–Penney lattice will generate scattered wave packets with the same characteristics as a single well. In particular the phenomenon of diffraction of wave packets in space and time [3] will apply to the lattice also. In section 4 we will show numerical calculations that support this claim and also depict scattering events for different numbers of wells at finite times in contrast to the results found here for long times.

4. Numerical results for the Kronig–Penney lattice

The following series of pictures depict the amplitude of the wavefunction obtained with the numerical algorithm described in [1]. We use Gaussian wells defined by

$$V(x) = -V_0 \sum_{n=0}^{N-1} \exp\left(-\frac{(x - x_n)^2}{b^2}\right) \tag{11}$$

where the equivalence to the square wells array of equation (7) is given by $b \approx \frac{w}{2}$. The impinging packet is a Gaussian wavepacket travelling from the left with an average speed v, initial location x_0, mass m, wave number $q = mv$ and width σ,

$$\psi = C \exp\left(\mathrm{i}q(x - x_0) - \frac{(x - x_0)^2}{4\sigma^2}\right). \tag{12}$$

We choose the parameters to be $V_0 = 1$ $a = 1$, $x_\mathrm{n} = 8$, $m = 20$, $q = 1$, $\sigma = 0.5$ and $x_0 = -20$, that implement the constraint of equation (6). In the case of a wider packet we find a smooth hump proceeding backwards and forwards [3].

Figures 1–3 show the backward scattered, the forward scattered and the well region wave amplitudes at $t = 15\,000$ for various numbers of wells.

The figures show clearly that the diffraction pattern that dominates the wave profile in the backward direction is the one of a single well, as expected from the results of section 3.

The amplitude of the wave is modulated by the diffraction pattern with the interference pattern appearing as oscillations inside each broad peak. The number of oscillations is identical to the number of wells, higher order interferences are blurred out into the background.

In figure 4 we depict a detail of the wave inside the 12th well for the case of 49 wells as compared to the wave for the case of a single scatterer. The behaviour is almost identical.

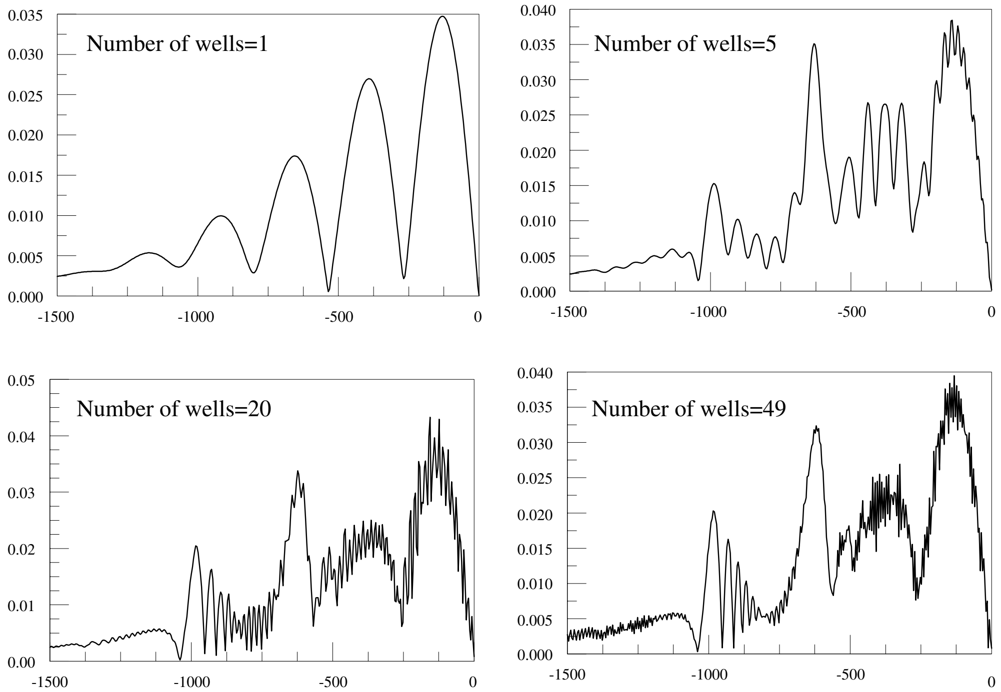

Figure 1. Wave amplitude in the backward region for different numbers of wells.

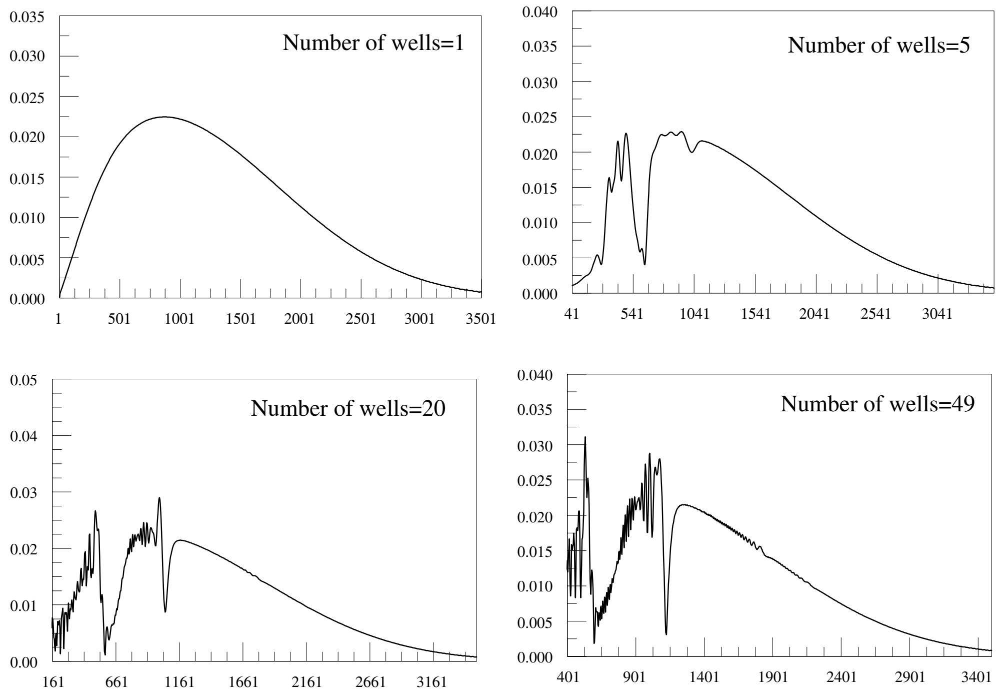

Figure 2. Wave amplitude in the forward region for different numbers of wells.

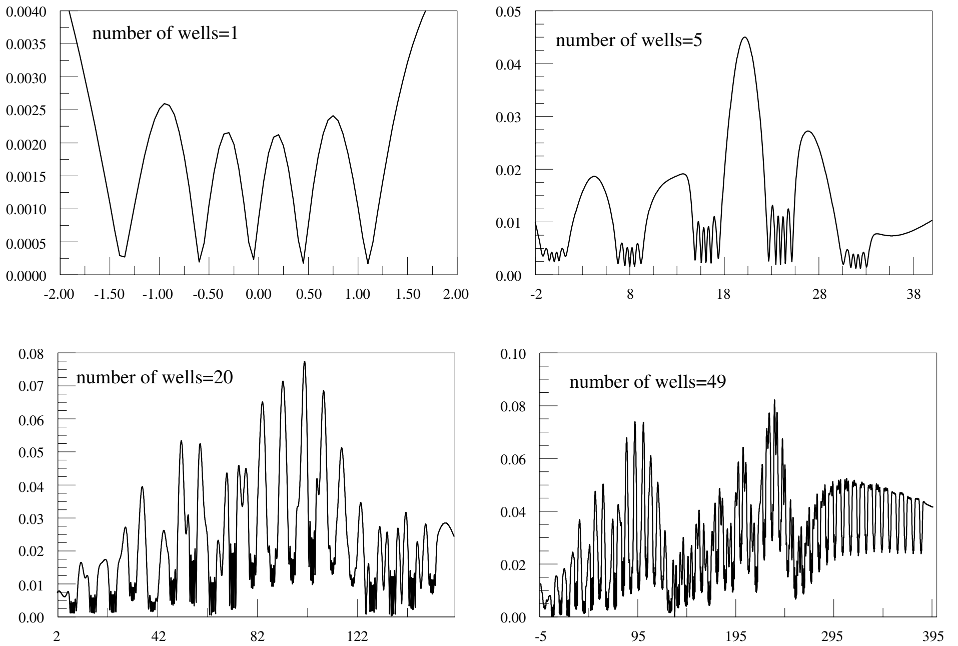

Figure 3. Wave amplitude in the well region for different numbers of wells.

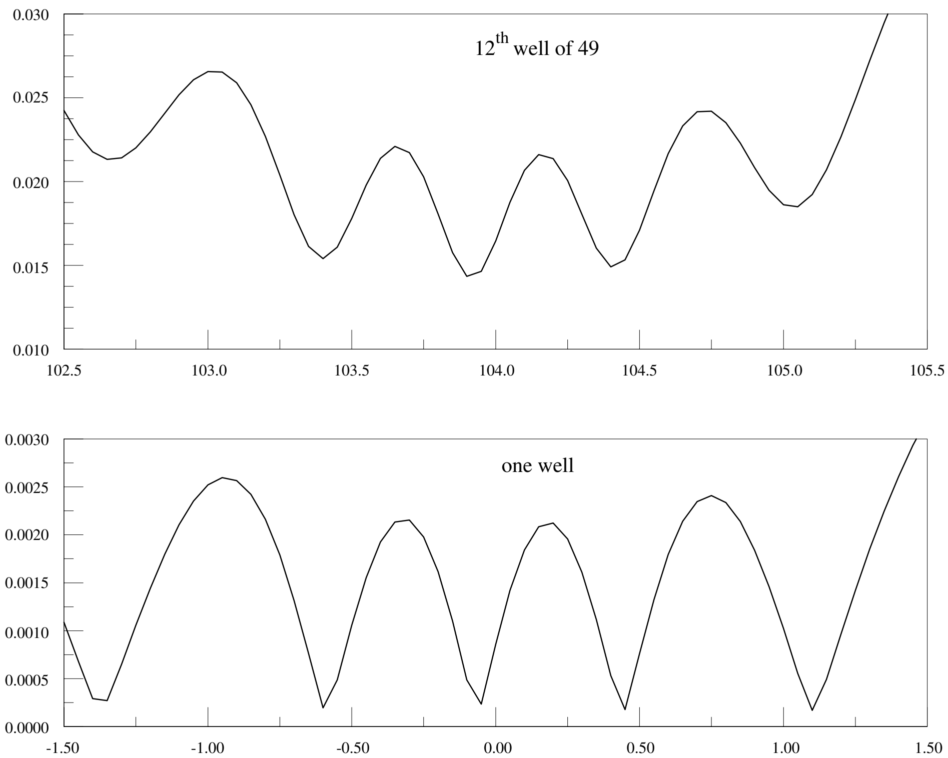

Figure 4. Detail of the wave amplitude inside a certain well.

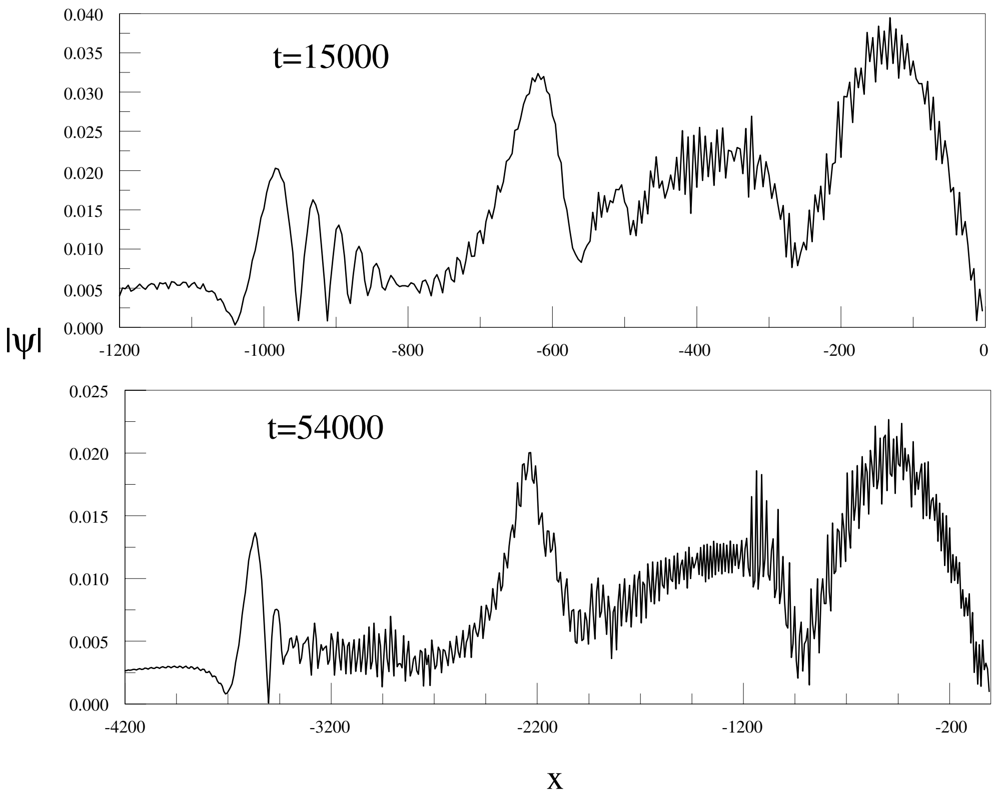

Figure 5. Wave amplitude in the backward region for 49 wells at different times.

The pattern repeats itself inside each well of the lattice, but the amplitude varies in space (well number) and time.

In section 3 we found that the long time behaviour should be dominated by the diffraction pattern of a single well. Therefore, the interference ripples should diminish as time elapses.

Figure 5 shows the results for a longer time and 49 wells. This calculation demanded almost a day of computer work. Further increase in the time makes the calculation prohibitive. However, this increase should be enough in order to see if there is a trend of dissipation of the interference ripples.

The disappearance of the broken peaks is most evident at long distance. At intermediate distances it is hard to assess if this is the case. We can expect that at even longer times the broken peaks will converge into the diffraction pattern humps broadening them to the size obtained with a single well.

5. Brief summary

We have found that the phenomenon of wave packet diffraction in space and time remains intact for a one-dimensional array of wells. On the experimental side, the present results suggest that besides the experiment simulated in [3] with helium it could be possible to use solid state devices, such as an array of quantum wells, to implement the effect. Future study will focus on the more realistic situation of a higher dimensional lattice of scatterers as well as other aspects of the newly found effect.

References

[1] Kälbermann G 1999 *Phys. Rev.* A **60** 2573
[2] Kälbermann G 2001 *J. Phys. A: Math. Gen.* **34** 3841
[3] Kälbermann G 2001 *J. Phys. A: Math. Gen.* **34** 6465
[4] Moshinsky M 1952 *Phys. Rev.* **88** 625
For more recent works see Xiao M 1999 *Phys. Rev.* E **60** 6226
[5] Brukner C and Zeilinger A 1997 *Phys. Rev.* A **56** 3804 and references therein
[6] Szriftgiser P, Guéry-Odelin D, Arndt M and Dalibard J 1997 *Phys. Rev. Lett.* **77** 4
[7] Kittel C 1996 *Introduction to Solid State Physics* (New York: Wiley)
[8] Bohm D 1951 *Quantum Theory* (Englewoods Cliffs, NJ: Prentice-Hall) p 259